Models for dielectrics at the continuum and molecular scales

L. Ridgway Scott
Departments of Computer Science and Mathematics,
Computation Institute, and Institute for Biophysical Dynamics,
University of Chicago

This talk is based on joint work with Ariel Ferndandez (Univ. of Wisconsin–Madison), Xie Dexuan (Univ. of Wisconsin–Milwaukee), Harold Scheraga (Cornell), and Kristina Rogale Plazonic (Princeton); and at U. Chicago: Steve Berry, Peter Brune, and Chris Fraser.

Dinosaurs at the University of Chicago

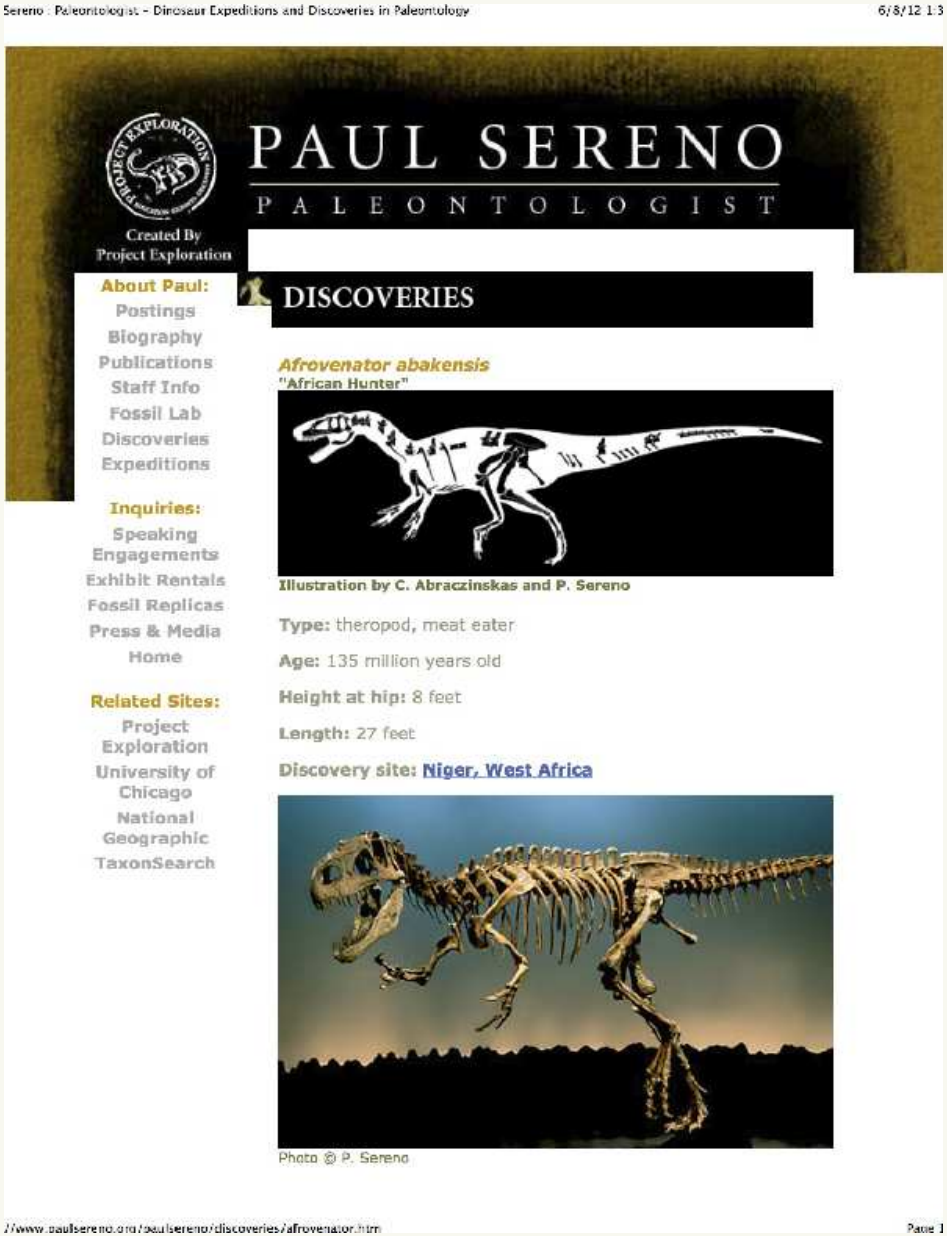

Paul Sereno (Professor in Organismal Biology and Anatomy, University of Chicago, Email: dinosaur@midway.uchicago.edu) has discovered the following dinosaurs:

Afrovenator abakensis
Carcharodontosaurus saharicus
Deltadromeus agilis
Eoraptor lunensis
Herrerasaurus ischigualastensis
Jobaria tiguidensis
Rajasaurus narmadensis
Rugops primus
Sarcosuchus imperator
Suchomimus tenerensis
The African Pterosaur

Different aspects of simulation

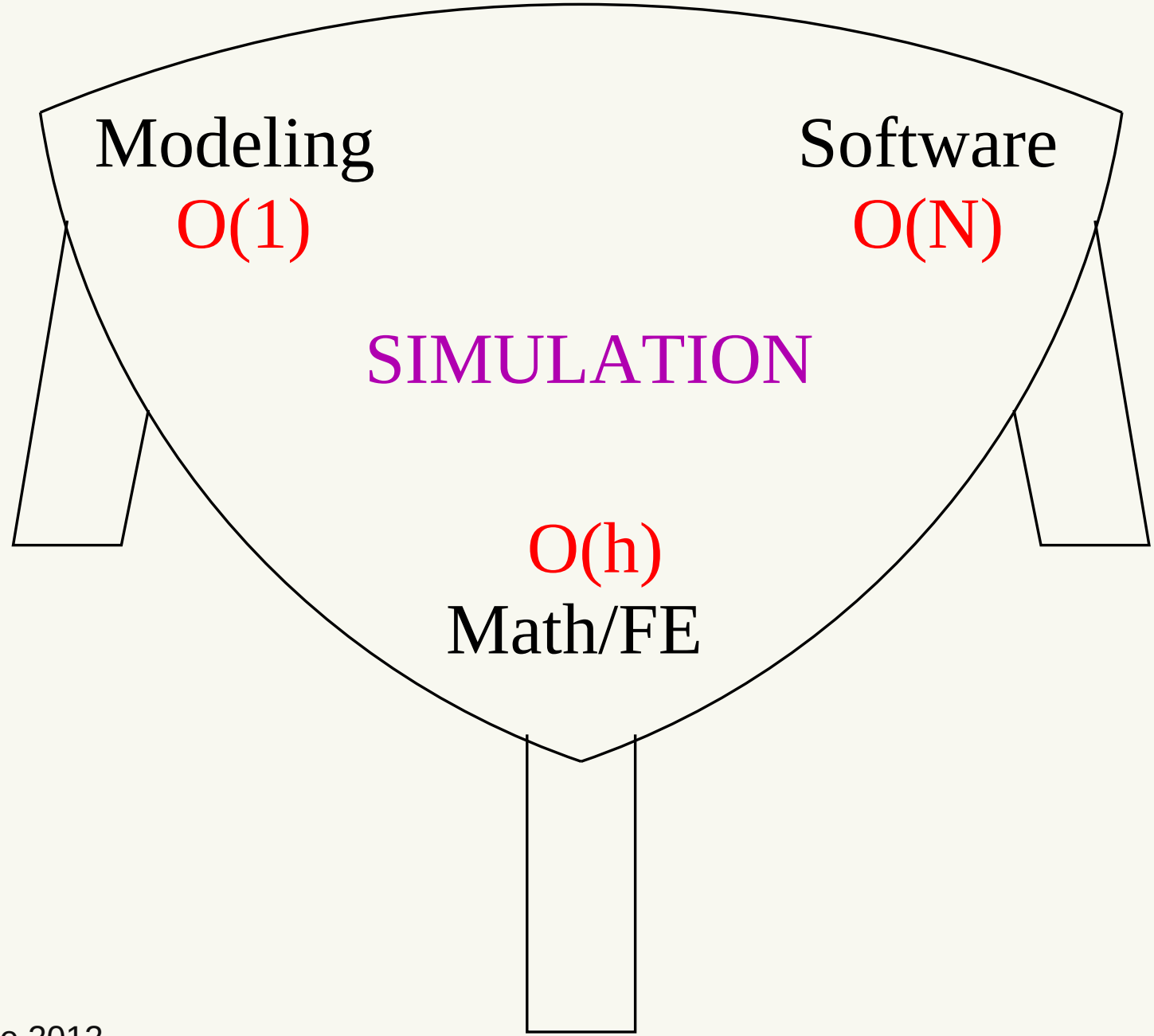

FEniCS uses math to generate code

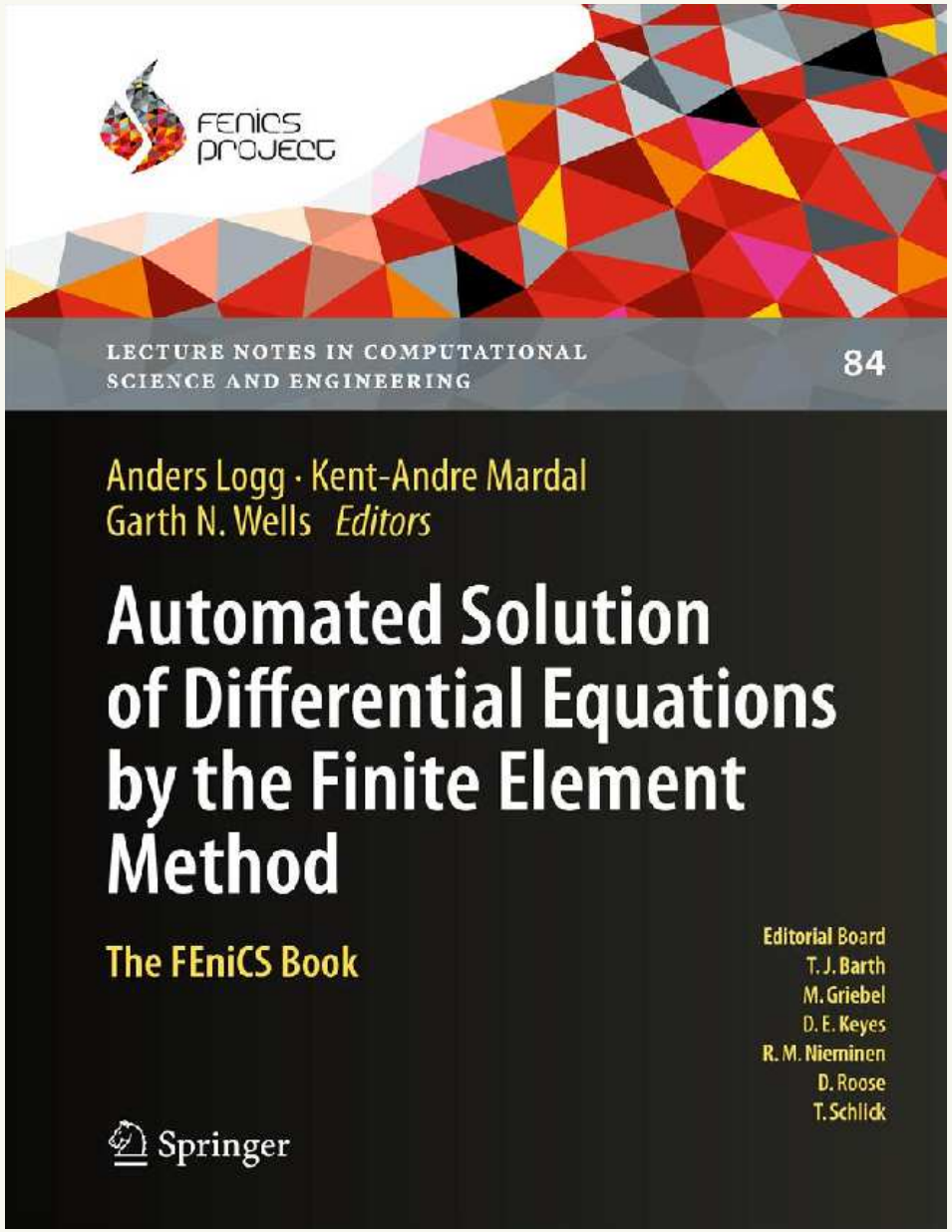

Different components of simulation software implement aspects of a different type of mathematical discipline.

FEniCS uses math to generate code

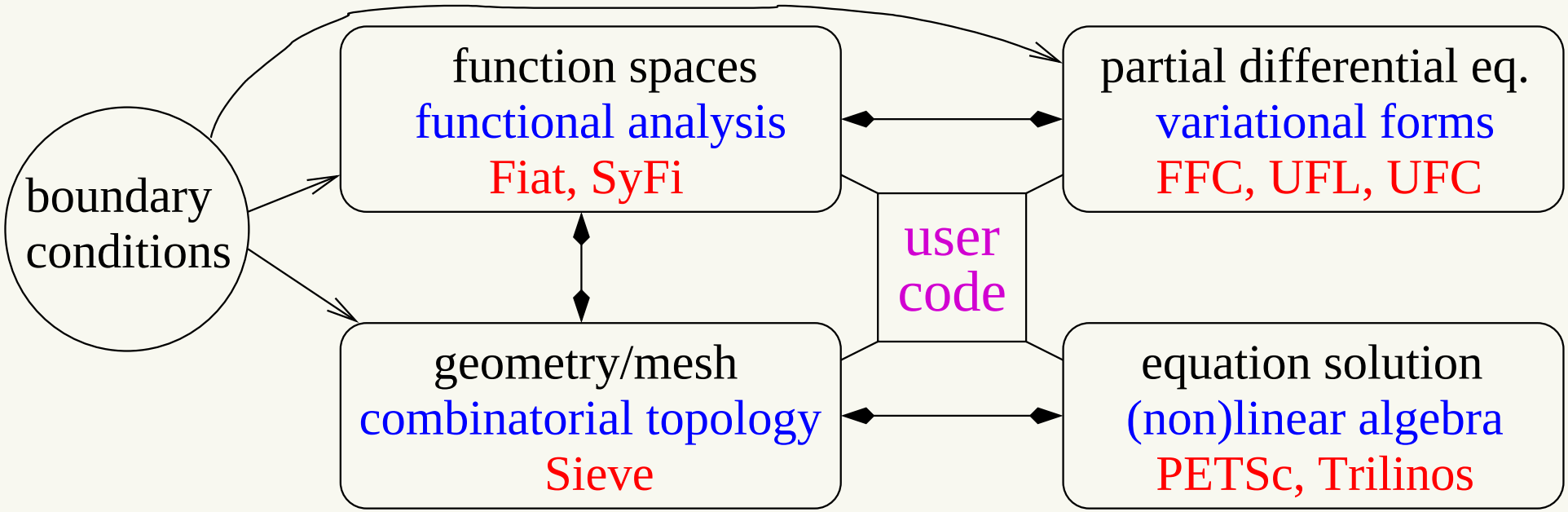

Figure 1: Different components of finite element codes and their default interactions. Mathematical description in blue, existing tools in red. The arrows indicate some of the interactions between different tools. Boundary conditions require interactions among three different tools.

For specificity, particular tools used in end-user codes from the FEniCS project are listed. Some of these tools have been developed within the FEniCS project, whereas others (e.g., PETSc, Trilinos) come from outside.

Protein sidechains have large electrostatic gradients

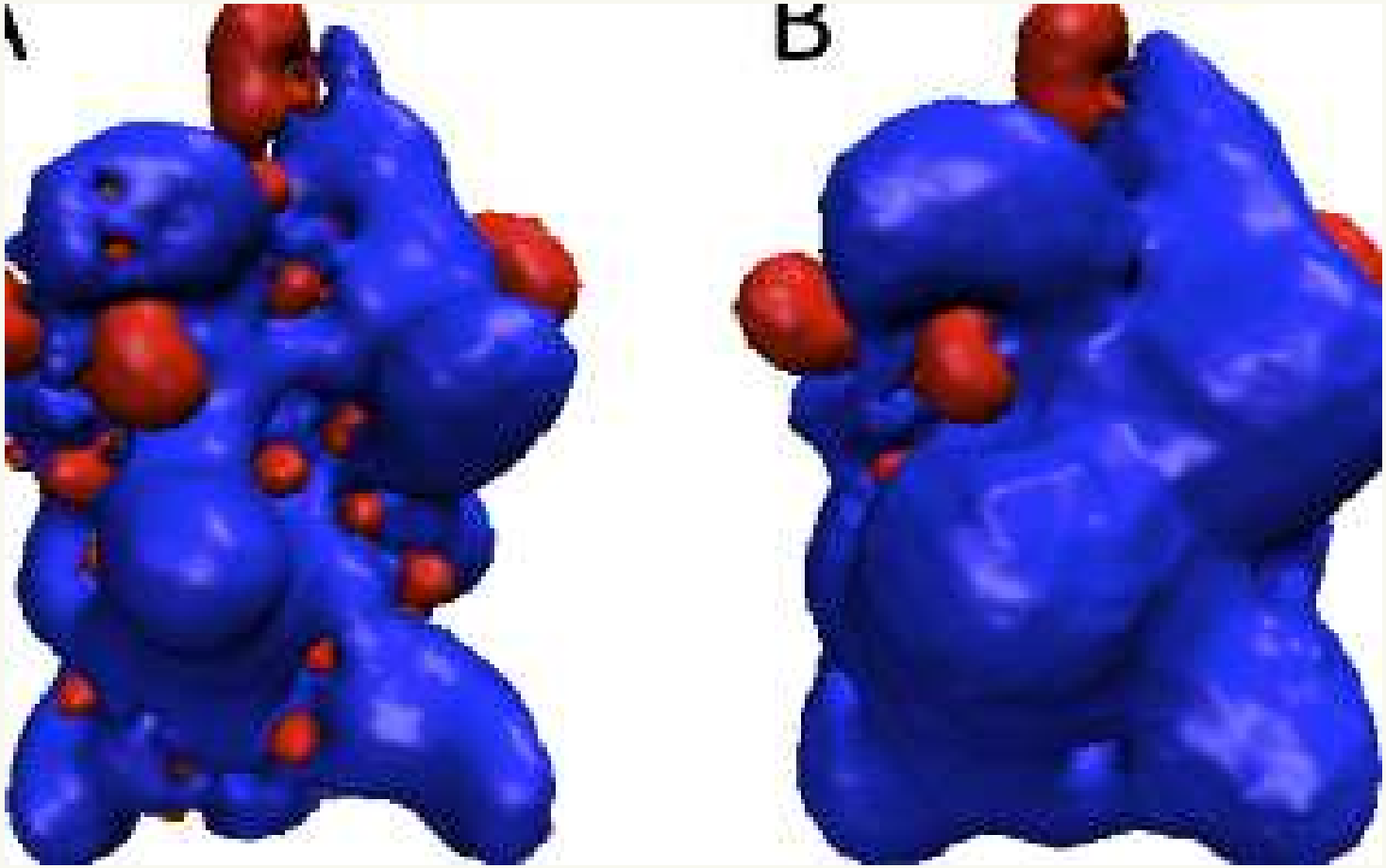

Figure 2: Different models suggest different modes of interactions. Shown are two nonlocal dielectric models with (A) and without (B) ionic effects.

Water forms a complicated network.

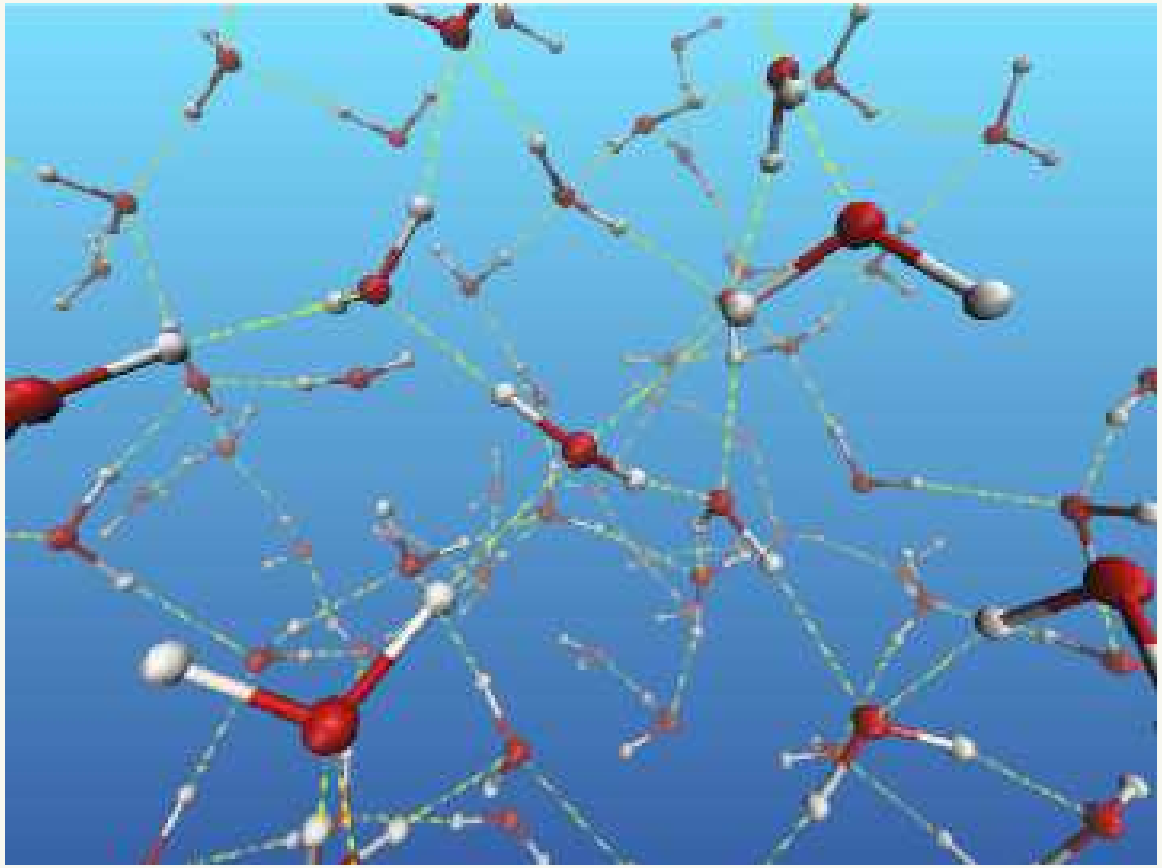

Figure 3: Water network from a molecular dynamics simulation.

Competing effects: why this is so hard

Protein sidechains have large electrostatic gradients

Water is a strong dielectric

Hydrophobic groups modify the water structure

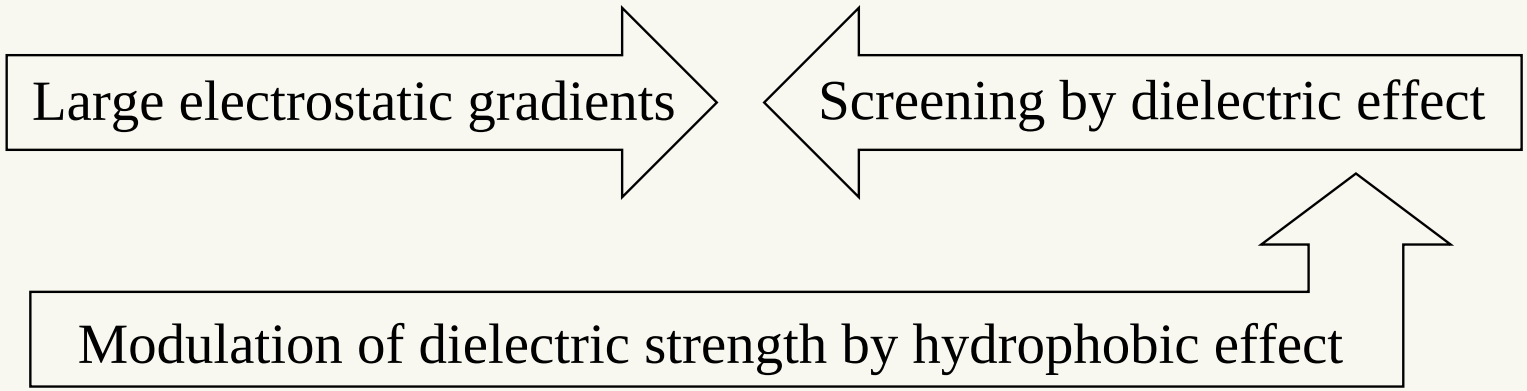

Figure 4: Three competing effects that determine protein behavior. These conspire to weaken interactive forces, making biological relationships more tenuous and amenable to mutation.

Charges in a dielectric are like lights in a fog.

Dielectric model

Consider two charge distributions ρ (fixed charges) and γ (polar groups free to rotate). Resulting electric potential ϕ satisfies

$$\Delta\phi = \rho + \gamma, \tag{1}$$

where the dielectric constant of free space is set to one.

Write $\phi = \phi_\rho + \phi_\gamma$, where $\Delta\phi_\gamma = \gamma$ and $\Delta\phi_\rho = \rho$.

Ansatz of Debye [4]: the electric field $\mathbf{e}_\gamma = \nabla\phi_\gamma$ is parallel to (opposing) the resulting electric field $\mathbf{e} = \nabla\phi$:

$$\nabla\phi_\gamma = (1 - \varepsilon)\nabla\phi. \tag{2}$$

Thus $\nabla\phi_\rho = \nabla\phi - \nabla\phi_\gamma = \varepsilon\nabla\phi$ and

$$\nabla \cdot (\varepsilon\nabla\phi) = \rho. \tag{3}$$

Polarization field and Debeye's Ansatz as projection

Define $\mathbf{p} = \nabla\phi_\gamma$: called the polarization field.

Recall $\mathbf{e} = \nabla\phi$.

Write $\mathbf{p} = (\epsilon - \epsilon_0)\mathbf{e} + \zeta\mathbf{e}^\perp$, so that

$$\epsilon = \epsilon_0 + \frac{\mathbf{p}\cdot\mathbf{e}}{\mathbf{e}\cdot\mathbf{e}},$$

with the appropriate optimism that $\mathbf{p} = 0$ when $\mathbf{e} = 0$.

That is, $\epsilon - \epsilon_0$ reflects the correlation between $\mathbf{p}$ and $\mathbf{e}$.

As defined, ϵ is a function of $\mathbf{r}$ and t, and potentially singular.

However, Debye postulated that a suitable average $\widetilde{\epsilon}$ should be well behaved:

$$\widetilde{\epsilon} = \epsilon_0 + \left\langle \frac{\mathbf{p}\cdot\mathbf{e}}{\mathbf{e}\cdot\mathbf{e}} \right\rangle .$$

Interpretation of ε

Manipulations leading to (3) valid when ε is an operator, even nonlinear.
In bulk water ε is a (temperature-dependent) constant:

$$\varepsilon \approx 87.74 - 40.00\,\tau + 9.398\,\tau^2 - 1.410\,\tau^3, \quad \tau \in [0, 1], \tag{4}$$

where $\tau = T/100$ and T is temperature in Centigrade (for $T > 0$) [5].
$\varepsilon >> 1$: opposing field strength $E_\gamma = \nabla\phi_\gamma$ much greater than inducing field.
ε increases with decreasing temperature; when water freezes, it increases further: for ice at zero degrees Centigrade, $\varepsilon \approx 92$.
But model fails when the spatial frequencies of the electric field $\nabla\phi$ are commensurate with the size of a water molecule, since the water molecules cannot orient appropriately to align with the field.
Thus frequency-dependent versions of ε have been proposed, and these are often called 'nonlocal' models since the operator ε must be represented either as a Fourier integral (in frequency space), or as an integral in physical space with a nonlocal kernel [2, 10].

Frequency dependence of dielectric constant

Debye observed that the effective permittivity is frequency dependent:

$$\epsilon(\nu) = \epsilon_0 + \frac{\epsilon_1 - \epsilon_0}{1 + \tau_D^2 \nu^2} \tag{5}$$

where τ_D is a characteristic time associated with the dielectric material and ν is the temporal wave number. Many experiments have verified this [8]:

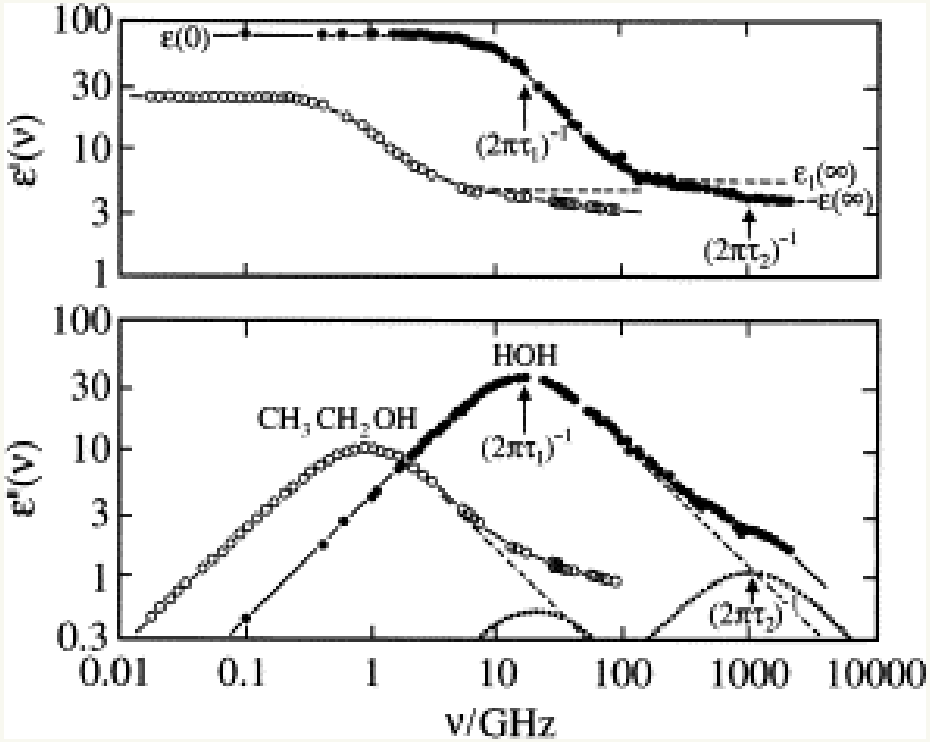

Polar residues cause spatial high frequencies

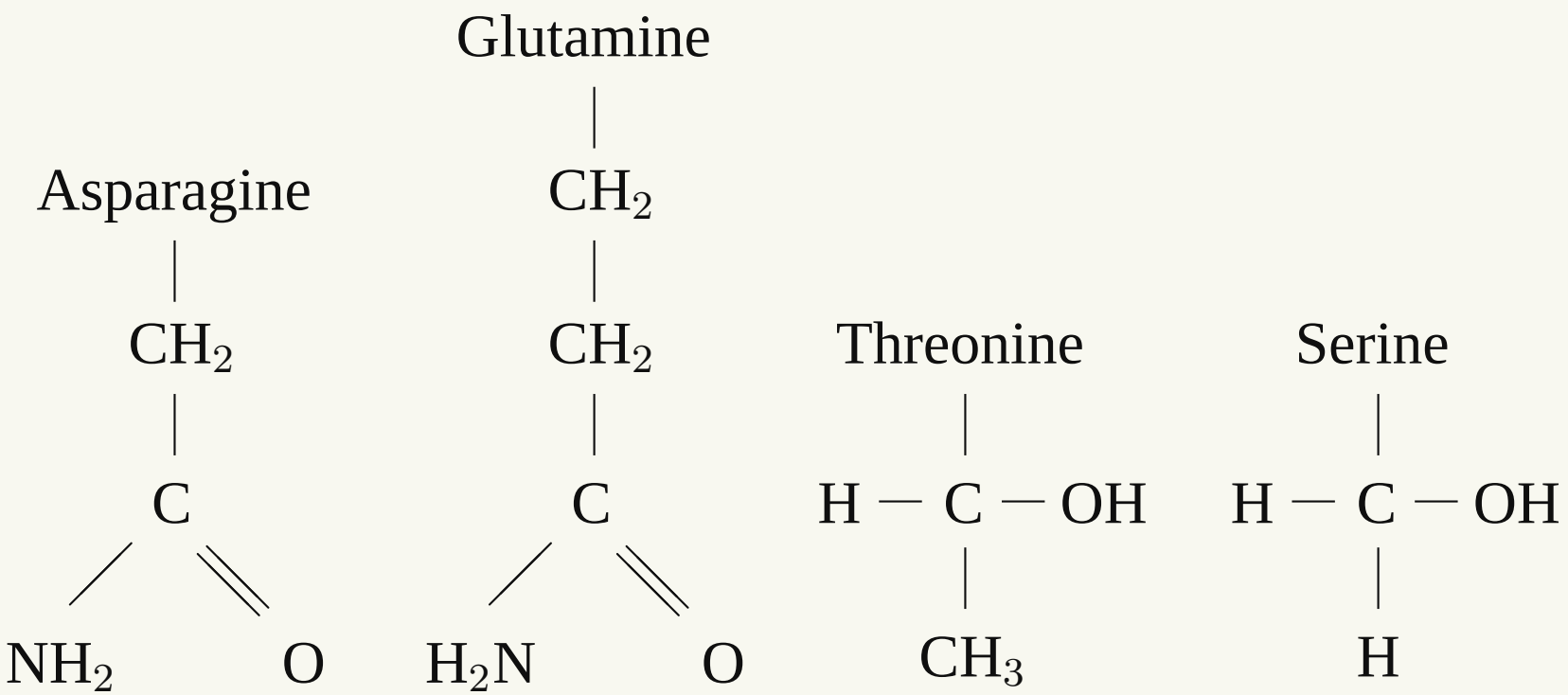

Some polar sidechains

Charged sidechains form salt bridge networks

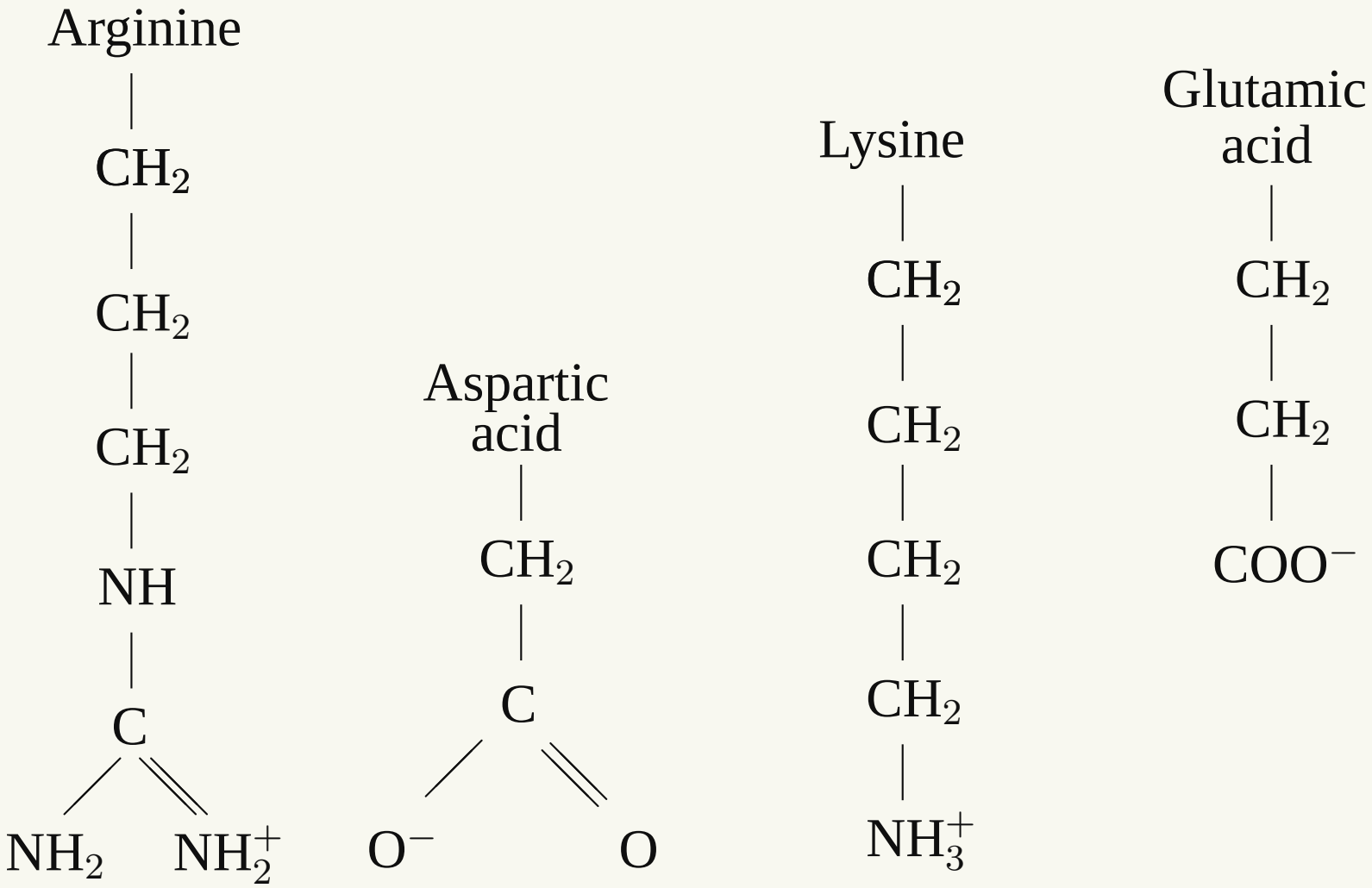

Charged sidechains

Nonlocal dielectric models

The nonlocal dielectric approach for estimating electrostatics was introduced by Dogonadze and Kornyshev [9] about fifteen years ago.

Since then, many studies have been done in the fields of chemistry, physics, and biology. A good review of these studies is given in [1].

Progress in the development of fast numerical algorithms was made by Hildebrandt [now at Mainz] *et al.* when they reformulated one commonly-used nonlocal electrostatic continuum model, called the Fourier-Lorentzian nonlocal model, as a system of coupled PDEs [6].

However, the Hildebrandt approach utilizes a complex splitting and certain jump terms, which we have been able to avoid.

Fourier-Lorentzian nonlocal model of water

Let $\Phi(\mathbf{r})$ denote the electrostatic potential function, and $\rho(\mathbf{r})$ be a given fixed charge density function. One commonly-used nonlocal dielectric model, called
the Fourier-Lorentzian nonlocal model, is defined by the integro-differential equation

$$\begin{cases} -\epsilon_0 \left[\epsilon_\infty \Delta\Phi(\mathbf{r}) + \frac{\epsilon_s - \epsilon_\infty}{\lambda^2} \nabla \cdot \int_{\mathbb{R}^3} H(\mathbf{r}-\mathbf{r}')\nabla\Phi(\mathbf{r}')\,\mathrm{d}\mathbf{r}'\right] = \rho(\mathbf{r}), & \mathbf{r} \in \mathbb{R}^3, \\ \Phi(\mathbf{r}) \to 0 & \text{as } |\mathbf{r}| \to \infty, \end{cases} \tag{6}$$

where ϵ_0 is the permittivity constant of the vacuum, ϵ_s is the permittivity factor for bulk water, ϵ_∞ is the permittivity factor for water in the limit of high frequency [11], λ is a positive parameter used to characterize the polarization correlations of water molecules, and $H(\mathbf{r})$ is the kernel function defined by

$$H(\mathbf{r}) = \frac{1}{4\pi|\mathbf{r}|} e^{-\frac{|\mathbf{r}|}{\lambda}}. \tag{7}$$

Free energy differences

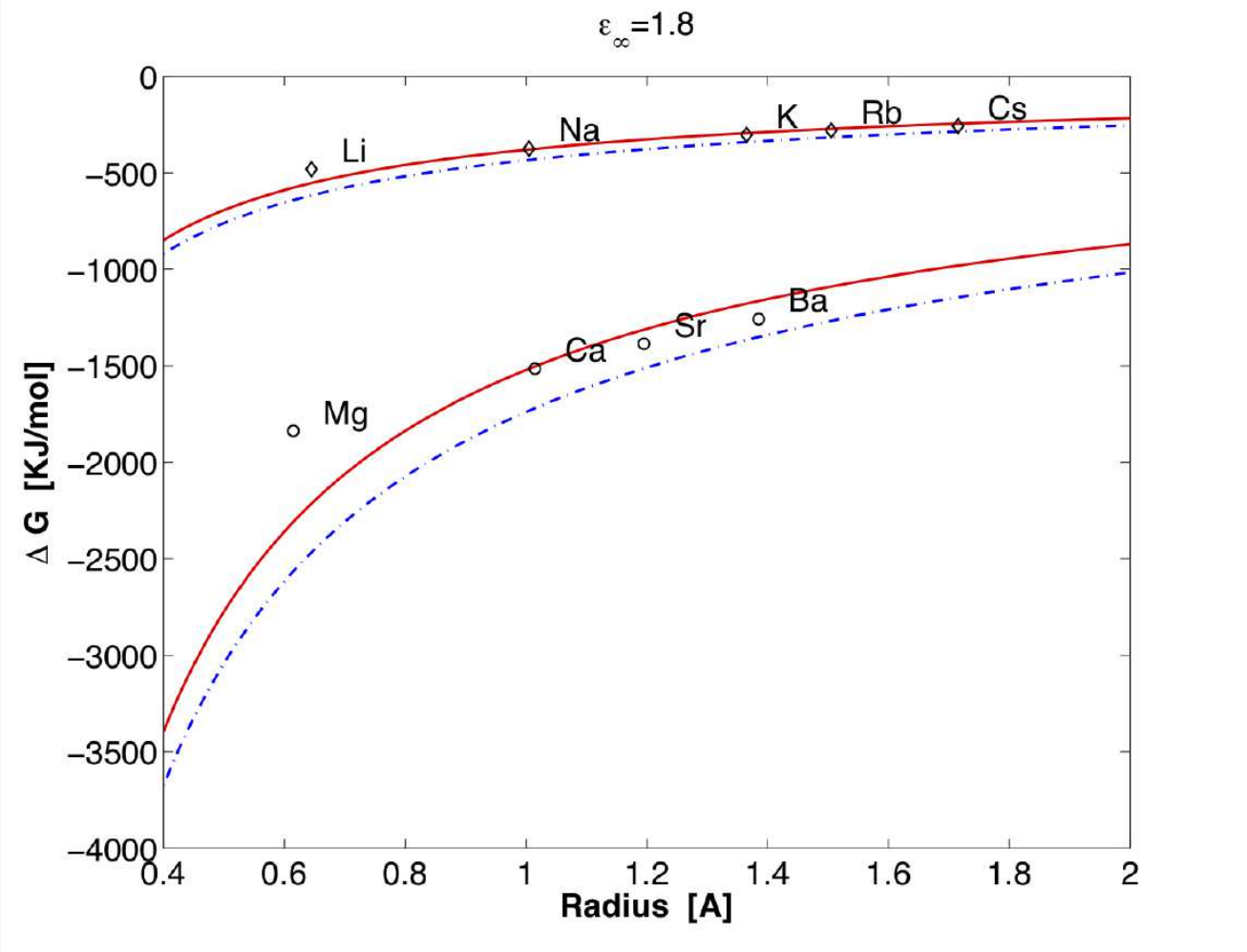

Figure 5: Comparisons of analytical free energy differences calculated from the nonlocal dielectric model with two values of λ ($\lambda = 15$Å and $\lambda = 30$Å) and the values from chemical experiments.

Caveats about the model

The nonlocal model is a much better predictor of important physical phenomena, such as the solvation free energy of ions (Figure 5).

Moreover, it is relatively insenstive to the choice of λ.

Shown in Figure 5 are results for the Born ion approximation for two values of λ that bracket the value $\lambda = 23$Å used in Hildebrandt's thesis [7].

The predicted results are remarkably accurate for most ions, espcially given the uncertainty in the ion radius.

However, they are very sensitive to the choice of ϵ_∞.

We are only accounting for the polar contribution to the free energy difference, and there is a nonpolar part that must also be estimated.

The main difficulty in solving the nonlocal model (6) comes from the integral term in which the integration and derivative are mixed together.

Key Step

A key step is to write the nonlocal dielectric model as an integro-differential equation in which the integral term involves only a convolution of the solution.

This new formulation leads to a fast finite element solver.

The convolution of the solution can be regarded as a unknown function, $u(\mathbf{r})$.

To calculate $u(\mathbf{r})$ we construct an "artificial" partial differential equation such that this equation has u as a solution and is coupled with the original equation of the nonlocal dielectric model.

In this way, the nonlocal dielectric model is reformulated into a system of two partial differential equations.
This approach can be naturally carried out in the framework of the Ritz-Galerkin variational formulation without involving any Helmholtz decomposition of the dielectric displacement field.
Hence, it is quite different from Hildebrandt *et al.*'s approach.

Simple splitting

Remarkably, we prove that there is a simple splitting of the system.

The electrostatic potential function $\Phi(\mathbf{r})$) can be split as a sum of two functions, with the property that these two functions can be found independently as the solutions of one Poisson equation and one Poisson-like equation each suitable for solution by a fast linear solver such as the multigrid method.

Using this solution splitting formula, we develop a finite element algorithm within the FEniCS framework.

Moreover, its computing cost is only double that of solving a classic Poisson dielectric model.

New algorithm

Note that $H(\mathbf{r})$ satisfies the following equation

$$-\Delta H + \frac{1}{\lambda^2} H = \delta, \tag{8}$$

where δ is the Dirac-delta distribution. Convolution on the both sides of (8) gives

$$(\Phi * \Delta H)(\mathbf{r}) = \frac{1}{\lambda^2}(\Phi * H)(\mathbf{r}) - \Phi(\mathbf{r}), \quad \mathbf{r} \in \mathbb{R}^3. \tag{9}$$

As a result, the integral term in (6) is simplified as

$$\nabla \cdot \int_{\mathbb{R}^3} H(\mathbf{r} - \mathbf{r}') \nabla \Phi(\mathbf{r}') \, \mathrm{d}\mathbf{r}' = \frac{1}{\lambda^2}(\Phi * H)(\mathbf{r}) - \Phi(\mathbf{r}), \quad \mathbf{r} \in \mathbb{R}^3,$$

so that the nonlocal model (6) can be reformulated into the new expression:

$$-\epsilon_\infty \Delta \Phi(\mathbf{r}) + \frac{\epsilon_s - \epsilon_\infty}{\lambda^2} \Phi(\mathbf{r}) - \frac{\epsilon_s - \epsilon_\infty}{\lambda^4}(\Phi * H)(\mathbf{r}) = \frac{1}{\epsilon_0} \rho(\mathbf{r}), \quad \mathbf{r} \in \mathbb{R}^n. \tag{10}$$

New solution splitting formula

Let Φ be the solution of the nonlocal model (6). Then it can be expressed as

$$\Phi(\mathbf{r}) = \frac{1}{\lambda^2 \epsilon_s}[(\epsilon_s - \epsilon_\infty) w(\mathbf{r}) + \epsilon_\infty v(\mathbf{r})], \quad \mathbf{r} \in \mathbb{R}^3, \tag{11}$$

where $w(\mathbf{r})$ and $v(\mathbf{r})$ are the functions satisfying the two Poisson-like equations:

$$\begin{cases} -\Delta w(\mathbf{r}) + \dfrac{\epsilon_s}{\lambda^2 \epsilon_\infty} w(\mathbf{r}) = \dfrac{\lambda^2}{\epsilon_0 \epsilon_\infty} \rho(\mathbf{r}), \quad \mathbf{r} \in \mathbb{R}^3, \\ w(\mathbf{r}) \to 0 \qquad \text{as } |\mathbf{r}| \to \infty, \end{cases} \tag{12}$$

and

$$\begin{cases} -\Delta v(\mathbf{r}) = \dfrac{\lambda^2}{\epsilon_0 \epsilon_\infty} \rho(\mathbf{r}), \quad \mathbf{r} \in \mathbb{R}^3, \\ v(\mathbf{r}) \to 0 \qquad \text{as } |\mathbf{r}| \to \infty. \end{cases} \tag{13}$$

Physics parameter values

Table 1: Physics parameter values used for computing free energy differences

Constant	Definition	Value
$\mathcal{N}_a$	Avogadro constant	6.022×10^{23}
ϵ_s	Permittivity ratio of bulk water	80 [5]
ϵ_∞	Permittivity ratio of confined water	1.8 [7], 2.34 [12]
ϵ_0	Permittivity of vacuum	8.854×10^{-12} [F/m]
$1e$	One electron charge	1.6×10^{-19} Coulomb

Free energy differences

Table 2: Free energy differences produced from chemical experiments for selected ions, together with the atomic radii and their uncertainties from Hildebrandt's thesis [7].

Ion	Radius of Born ball [Å]	Charge [e]	Free energy [KJ/mol]
Na^+	1.005 ± 0.04	1	-375
K^+	1.365 ± 0.05	1	-304
Ca^{2+}	1.015 ± 0.02	2	-1515
Sr^{2+}	1.195	2	-1386

Nonlinear models

Polarization field $\nabla\phi_\gamma$ saturates for large fixed fields:

$$\lim_{|\nabla\phi|\to\infty}(1-\varepsilon)\nabla\phi = \lim_{|\nabla\phi|\to\infty}\nabla\phi_\gamma = C, \tag{14}$$

One simple model that satisfies (14) is

$$\varepsilon(x) = \varepsilon_0 + \frac{\varepsilon_1}{1+\lambda|\nabla\phi(x)|} \tag{15}$$

for some constants ε_0, ε_1, and λ.

Both the nonlocal and nonlinear models of the dielectric response have the effect of representing frequency dependence of the dielectric effect.

$|\nabla\phi(x)|$ provides a proxy for frequency content, although it will not reflect accurately high-frequency, low-power electric fields.

Combination of nonlocal and nonlinear dielectric models may be needed.

Local model for dielectric effect?

Hydrophobic (CH_n) groups remove water locally.

This causes a reduction in ε locally.
(Resulting increase in ϕ makes dehydrons sticky.)

This can be quantified and used to predict binding sites.

The placement of hydrophobic groups near an electrostatic bond is called wrapping.

Like putting insulation on an electrical wire.

(Wrapping modifies dielectric effect)

We can see this effect on a single hydrogen bond.

Wrapping protects hydrogen bond from water

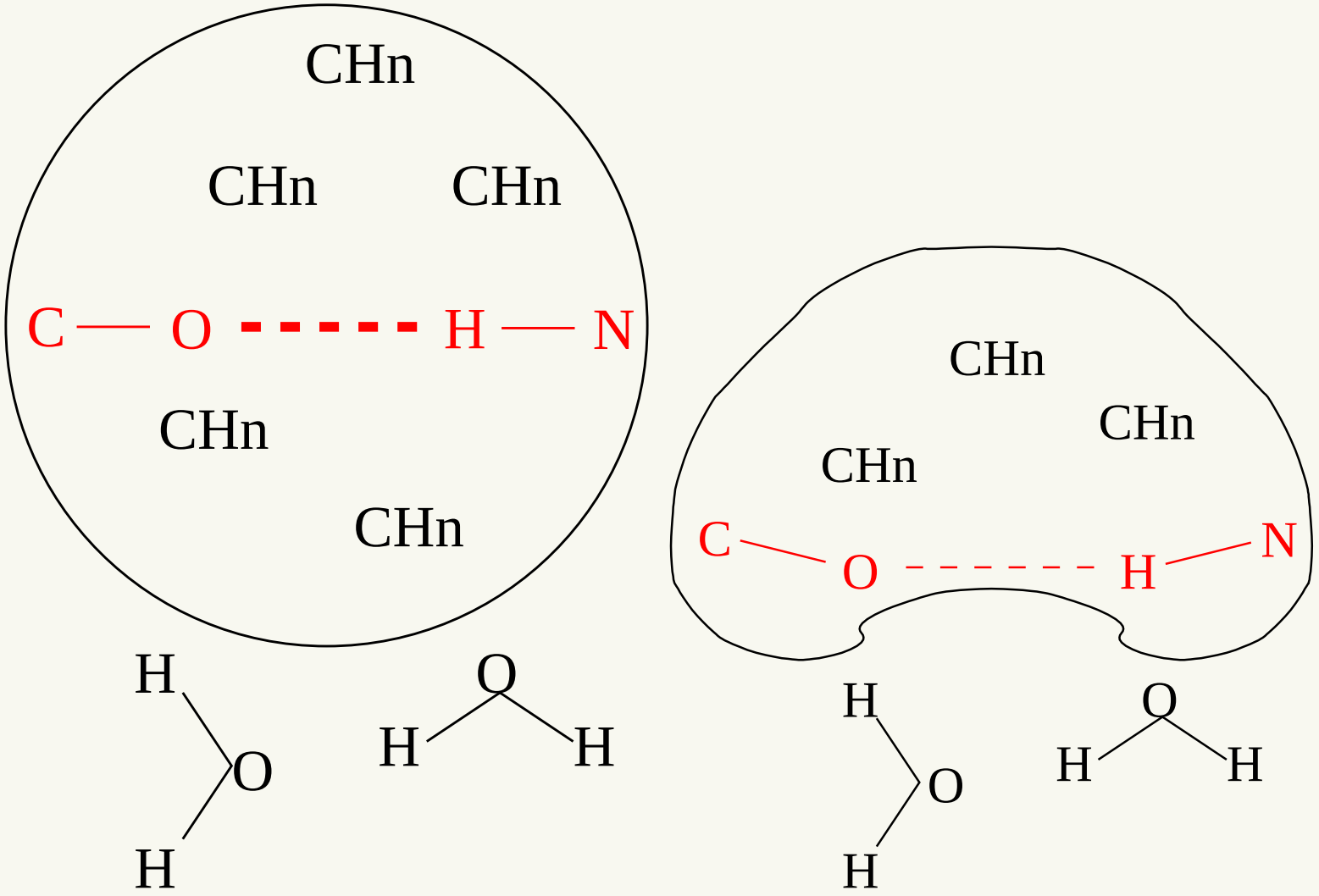

Well wrapped hydrogen bond Underwrapped hydrogen bond

Extent of wrapping changes nature of hydrogen bond

Hydrogen bonds (B) that are not protected from water do not persist.

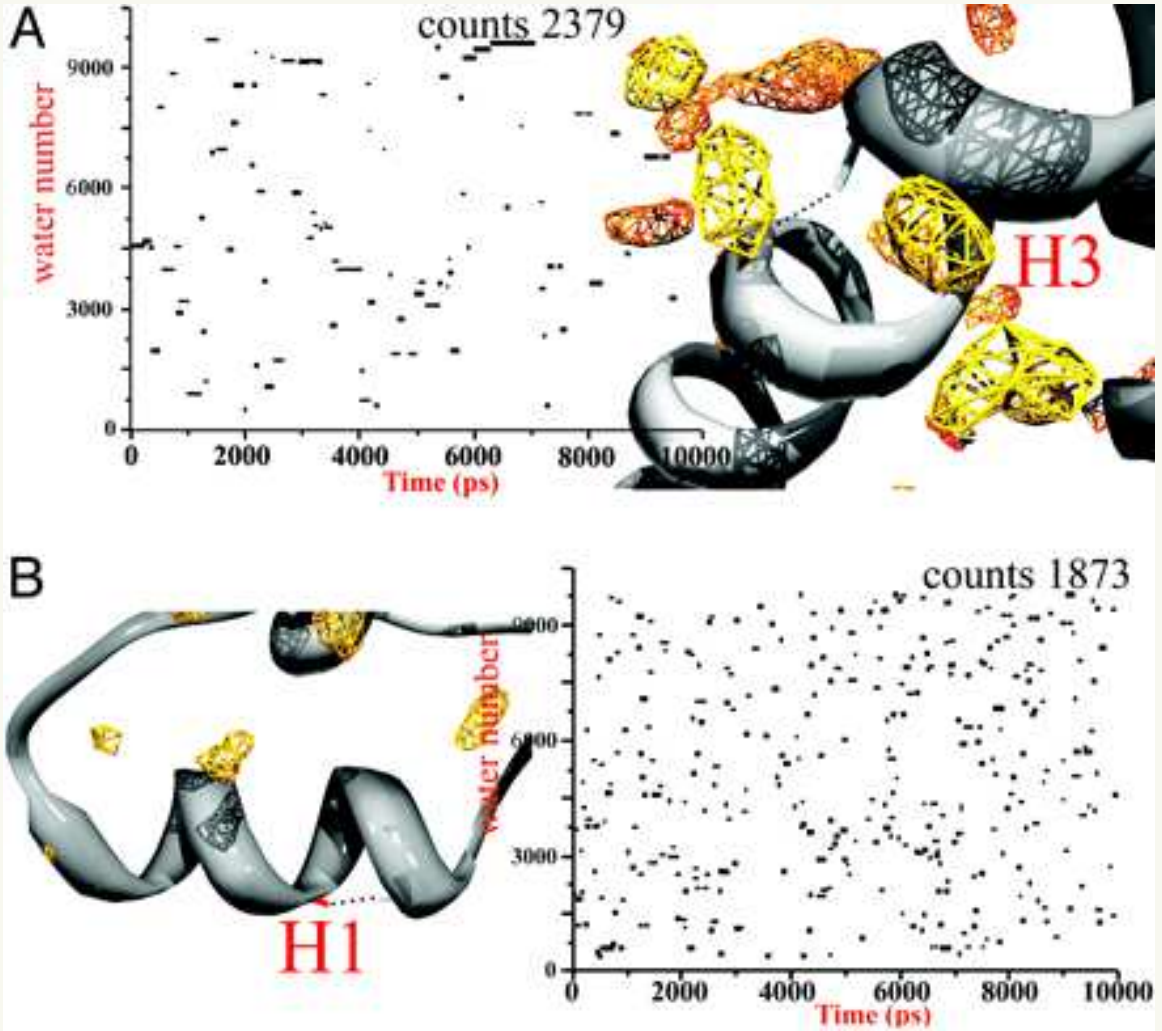

From De Simone, et al., PNAS 102 no 21 7535-7540 (2005)

Dynamics of hydrogen bonds and wrapping

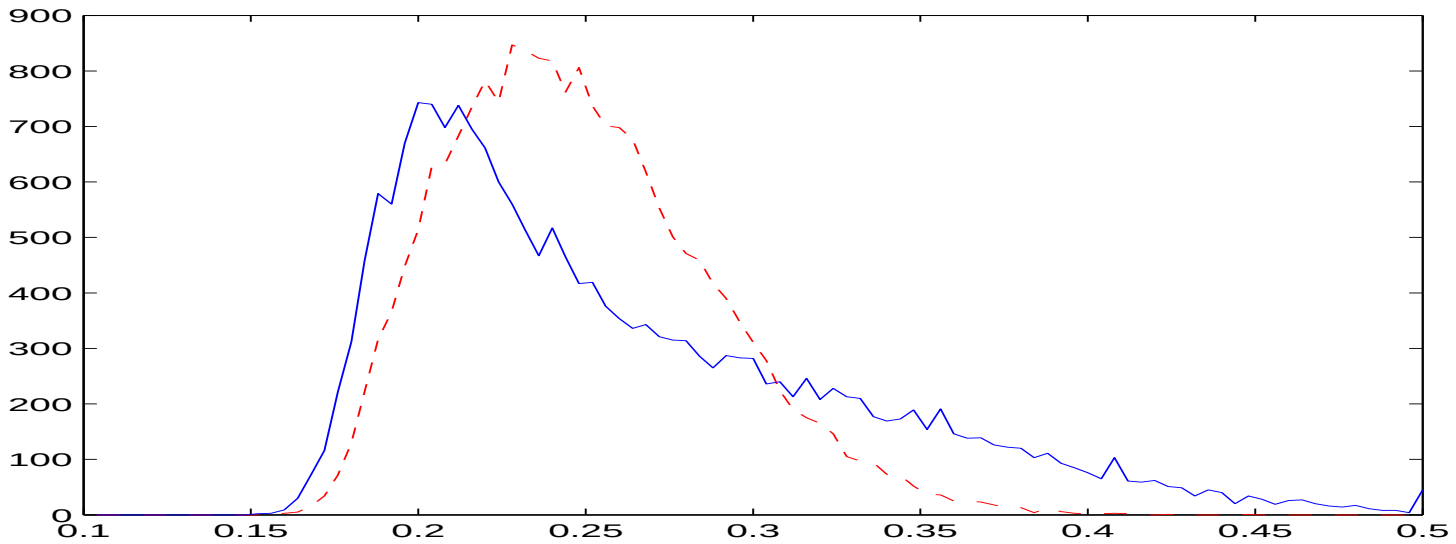

Figure 6: Distribution of bond lengths for two hydrogen bonds formed in a structure of the sheep prion [3]. Horizontal axis measured in nanometers, vertical axis represents numbers of occurrences taken from a simulation with $20,000$ data points with bin widths of 0.1 Ångstrom. Distribution for the well-wrapped hydrogen bond (H3) has smaller mean value but a longer (exponential) tail, whereas distribution for the underwrapped hydrogen bond

Ligand binding removes water

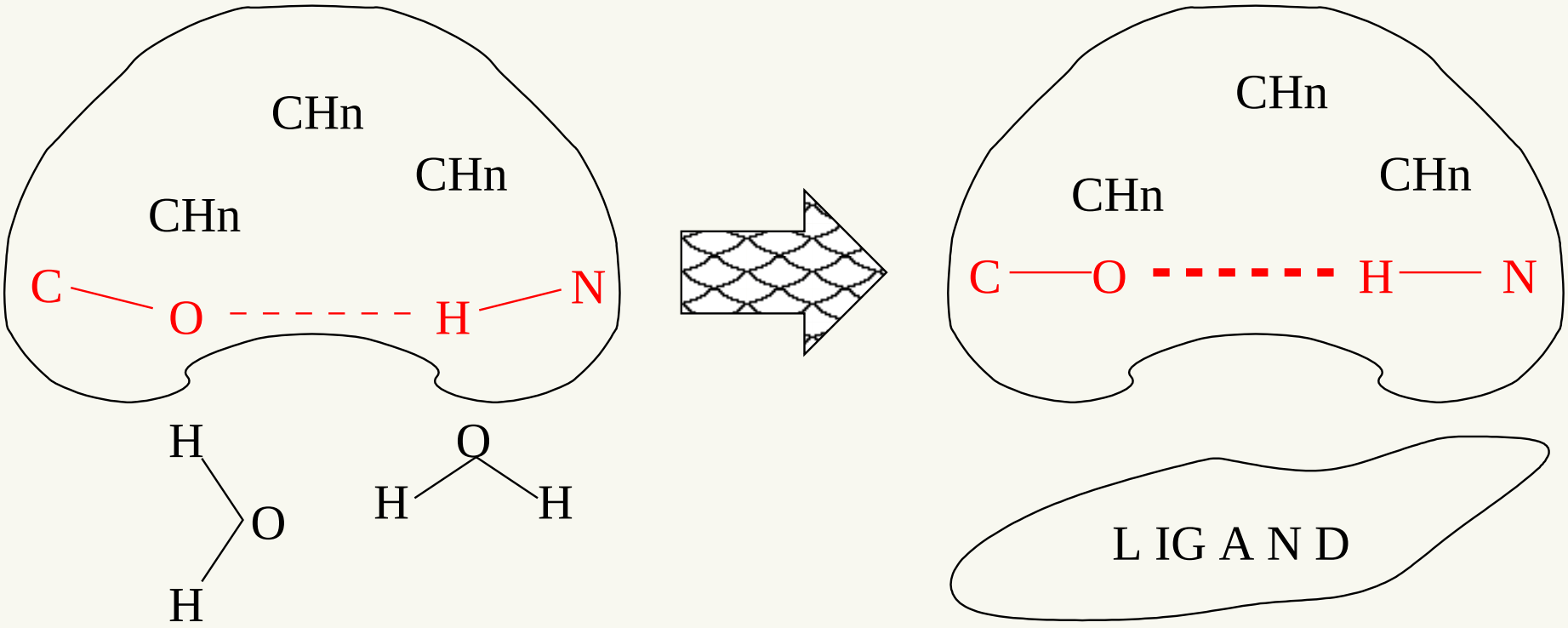

Binding of ligand changes underprotected hydrogen bond (high dielectric) to strong bond (low dielectric)

No intermolecular bonds needed!

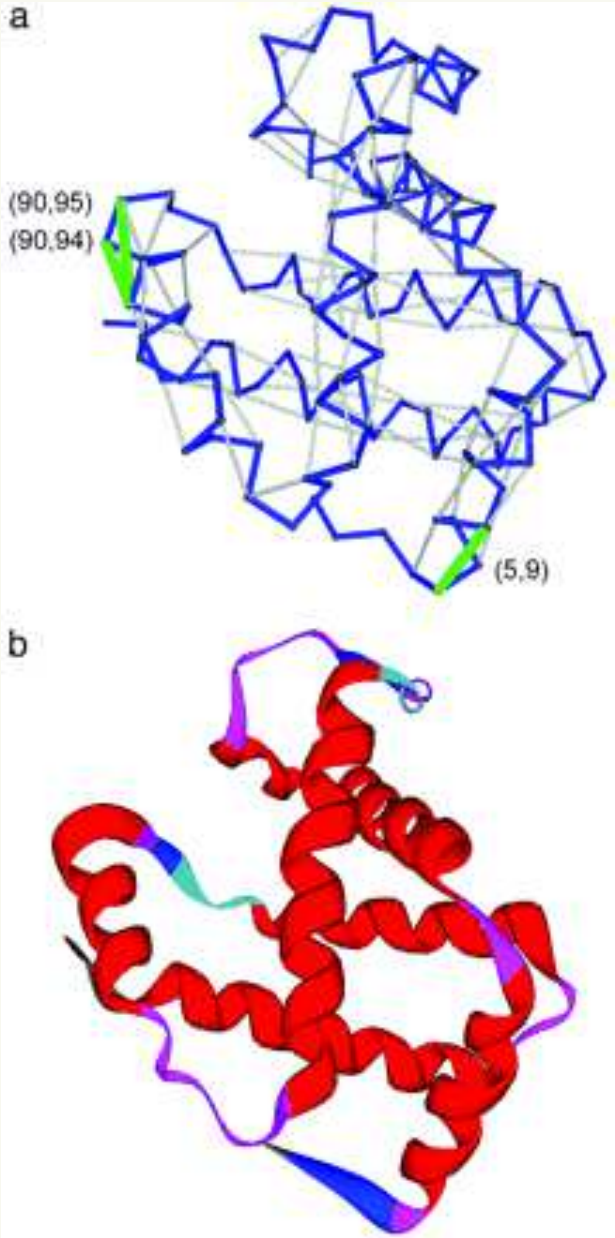

Dehydrons

in human hemoglobin, From PNAS 100: 6446-6451 (2003) Ariel Fernandez, Jozsef Kardos, L. Ridgway Scott, Yuji Goto, and R. Stephen Berry. Structural defects and the diagnosis of amyloidogenic propensity.

Well-wrapped hydrogen bonds are grey, and dehydrons are green.

The standard ribbon model of “structure” lacks indicators of electronic environment.

Antibody binding to HIV protease

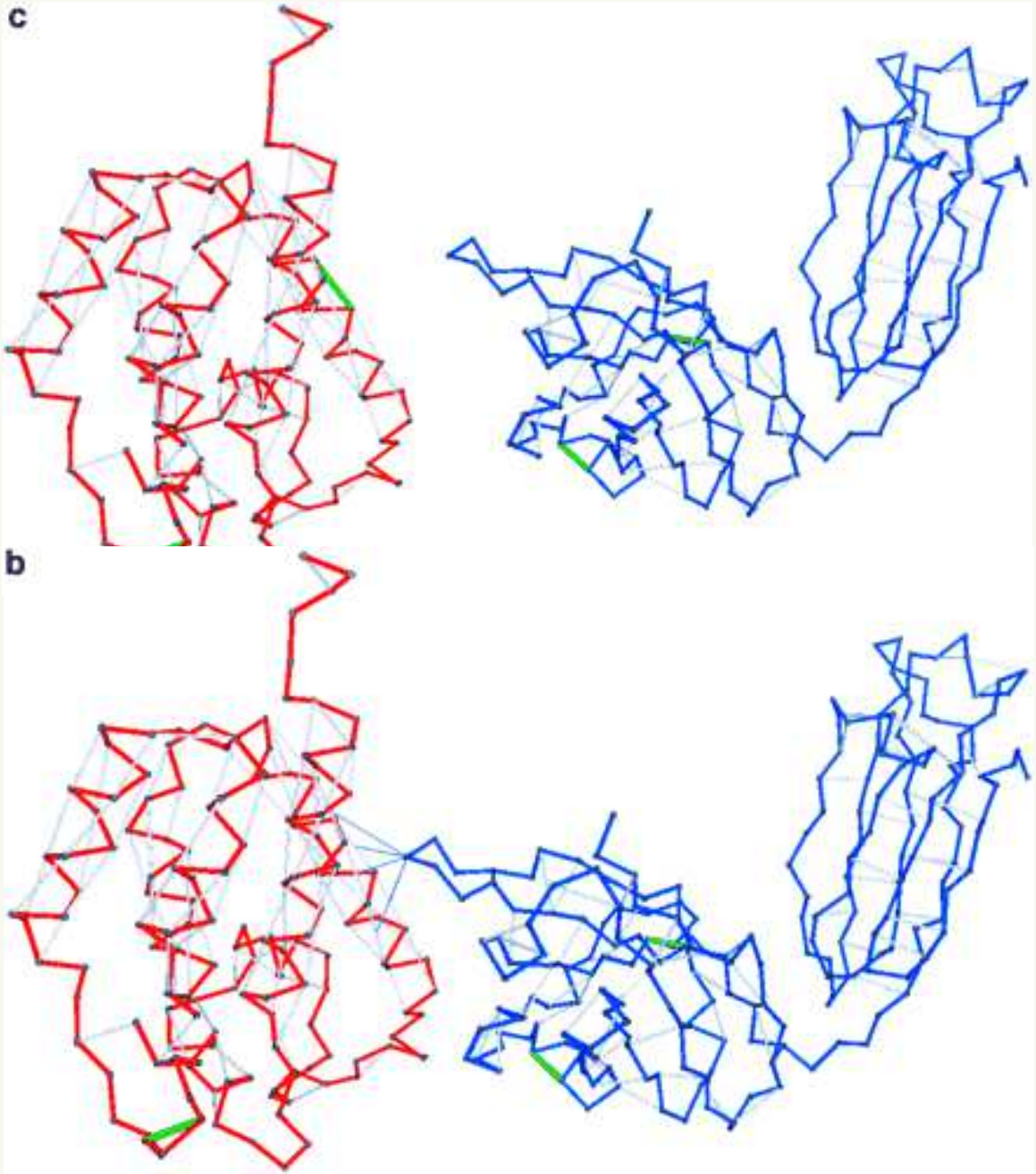

The HIV protease has a dehydron at an antibody binding site.

When the antibody binds at the dehydron, it wraps it with hydrophobic groups.

A model for protein-protein interaction

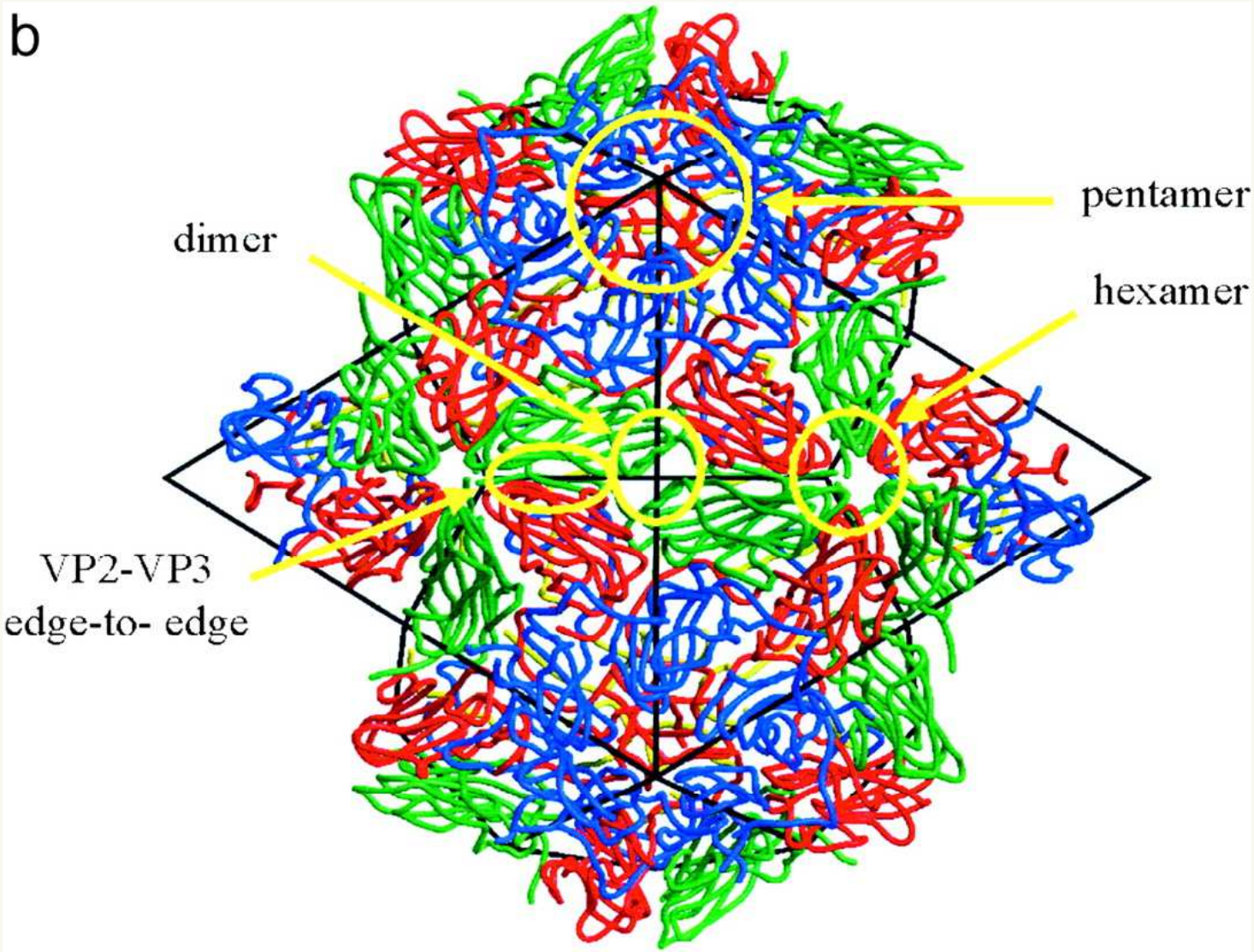

Foot-and-mouth disease virus assembly from small proteins.

Dehydrons guide binding

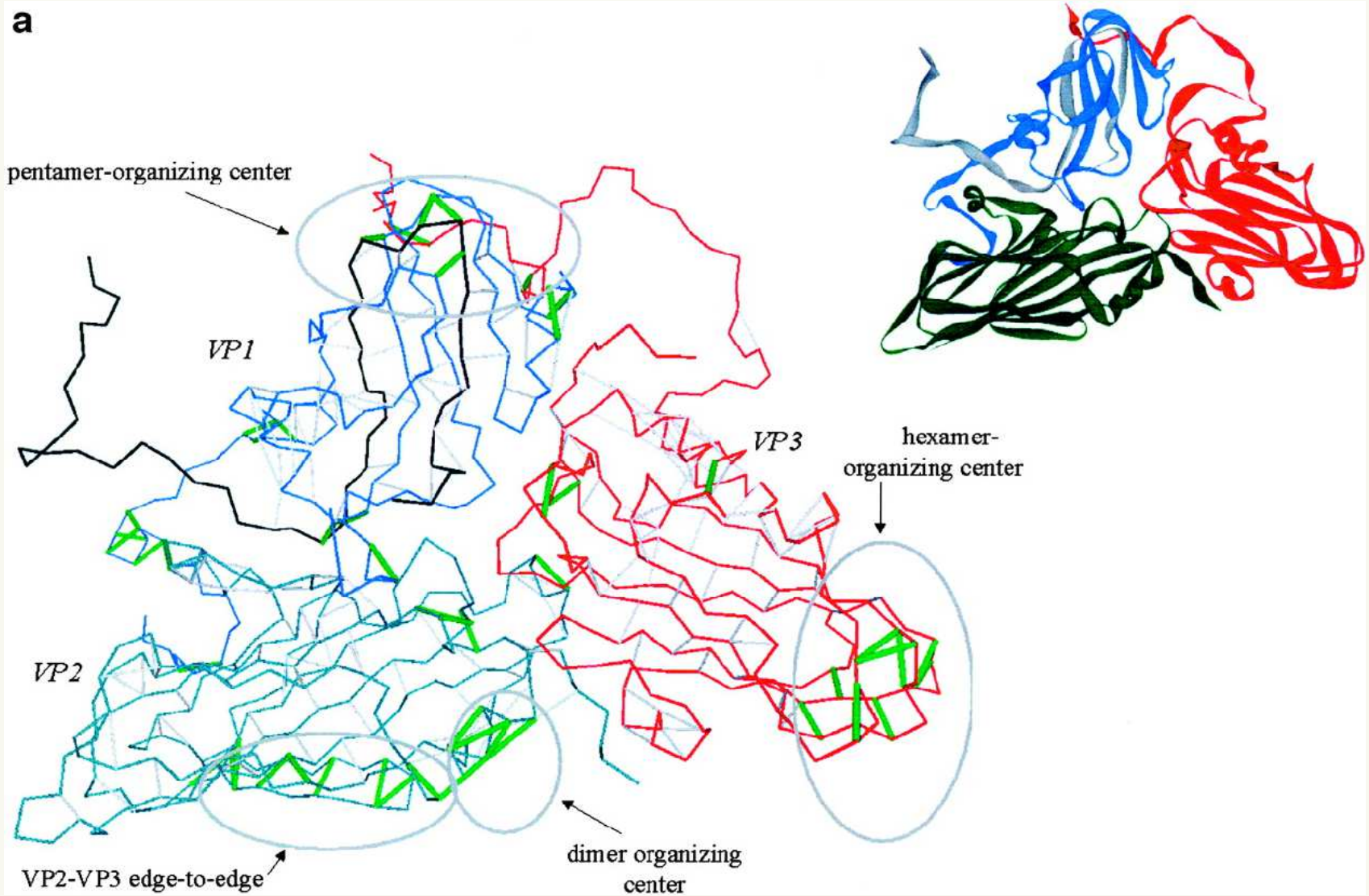

Dehydrons guide binding of component proteins VP1, VP2 and VP3 of foot-and-mouth disease virus.

References

[1] V. Basilevsky and G. N. Chuev. Nonlocal solvation theories. In Benedetta Mennucci and Roberto Cammi, editors, *Continuum Solvation Models in Chemical Physics: From Theory to Applications*. Wiley, 2008.

[2] P. A. Bopp, A. A. Kornyshev, and G. Sutmann. Static nonlocal dielectric function of liquid water. *Physical Review Letters*, 76:1280–1283, 1996.

[3] Alfonso De Simone, Guy G. Dodson, Chandra S. Verma, Adriana Zagari, and Franca Fraternali. Prion and water: Tight and dynamical hydration sites have a key role in structural stability. *Proceedings of the National Academy of Sciences, USA*, 102:7535–7540, 2005.

[4] P. Debye. *Polar Molecules*. Dover, New York, 1945.

[5] John Barrett Hasted. *Aqueous Dielectrics*. Chapman and Hall, 1974.

[6] A. Hildebrandt, R. Blossey, S. Rjasanow, O. Kohlbacher, and H.-P. Lenhof. Novel formulation of nonlocal electrostatics. *Physical Review Letters*, 93(10):108104, Sep 2004.

[7] Andreas Hildebrandt. *Biomolecules in a structured solvent: A novel formulation of nonlocal electrostatics and its numerical solution*. PhD thesis, Universität des Saarlandes, 2005.

[8] U. Kaatze, R. Behrends, and R. Pottel. Hydrogen network fluctuations and dielectric spectrometry of liquids. *Journal of Non-Crystalline Solids*, 305(1):19–28, 2002.

[9] Alexei A. Kornyshev and Godehard Sutmann. Nonlocal dielectric saturation in liquid water. *Physical Review Letters*, 79:3435–3438, 1997.

[10] L. Ridgway Scott, Mercedes Boland, Kristina Rogale, and Ariel Fernández. Continuum equations for dielectric response to macro-molecular assemblies at the nano scale. *Journal of Physics A: Math. Gen.*, 37:9791–9803, 2004.

[11] GJ Wilson, RK Chan, DW Davidson, and E. Whalley. Dielectric properties of ices II, III, V, and VI. *Journal of Chemical Physics*, 43:2384, 1965.